

This is the pre-peer reviewed version of the following article: *Granados-Fitch, MG, Quintana-Melgoza, JM, Juarez-Arellano, EA, Avalos-Borja, M. Chemical stability of superhard rhenium diboride at oxygen and moisture ambient environmental conditions prepared by mechanical milling. J Am Ceram Soc. 2018; 101: 3148– 3155*, which has been published in final form at: <https://doi.org/10.1111/jace.15461> This article may be used for non-commercial purposes in accordance with Wiley Terms and Conditions for Use of Self-Archived Versions

**Chemical stability of superhard rhenium diboride at oxygen and moisture ambient  
environmental conditions prepared by mechanical milling**

Mizraim G. Granados-Fitch<sup>a</sup>, Juan M. Quintana-Melgoza<sup>b</sup>, Erick A. Juarez-Arellano<sup>c</sup>, Miguel  
Avalos-Borja<sup>a,\*</sup>

<sup>a</sup>División de Materiales Avanzados, Instituto Potosino de Investigación Científica y Tecnológica,  
San Luis Potosí, San Luis Potosí 78216, México.

<sup>b</sup>Facultad de Ciencias Químicas e Ingeniería, Universidad Autónoma de Baja California, Tijuana,  
Baja California 22390, México.

<sup>c</sup>Instituto de Química Aplicada, Universidad del Papaloapan, San Juan Bautista Tuxtepec,  
Oaxaca 68301, México.

Abstract

In this study, rhenium diboride ( $\text{ReB}_2$ ) was obtained by mechanosynthesis at 640 min of milling. The obtained  $\text{ReB}_2$  was stored at oxygen and moisture ambient environmental conditions in order to know the chemical stability. The results indicate that  $\text{ReB}_2$  is totally decomposed at oxygen and moisture ambient environmental conditions. Further, the XRD analysis of  $\text{ReB}_2$  samples after 26 months of storage shows that the final products of degradation are  $\text{HReO}_4$  (liquid),  $\text{H}_3\text{BO}_3$ ,  $\text{HBO}_2$  and  $\text{ReO}_3$ . Finally, a schematic diagram of the degradation sequence of  $\text{ReB}_2$  at oxygen and moisture ambient environmental conditions is proposed and validated with a thermodynamic analysis.

Keywords: rhenium diboride; octahedral particles; mechanosynthesis; degradation

\*miguel.avalos@ipicyt.edu.mx (M. Avalos Borja).

## 1. Introduction

Hard and superhard materials such as nitrides, carbides and borides of transition metals, as well as cubic boron nitride and diamond have been used in many applications where high hardness, incompressibility and chemical inertness are priorities.<sup>1</sup> Rhenium diboride ( $\text{ReB}_2$ ) was synthesized for the first time in 1962, its crystalline structure is hexagonal with  $a=0.2900$  nm and  $c=0.7478$  nm, with two  $\text{ReB}_2$  units per unit cell.<sup>2</sup> Recently,  $\text{ReB}_2$  has been classified as a superhard and incompressible material because it has hardness (20 to 60 GPa),<sup>3-8, 12</sup> bulk modulus (173 to 371 GPa),<sup>3-6, 9-11</sup> Young modulus (382-712 GPa)<sup>5, 6, 10</sup> and incompressibility along the  $c$  axis ( $00l$  planes),<sup>4</sup> therefore, it has been proposed as material to be used in cutting and grinding tools. As was mentioned previously, the  $\text{ReB}_2$  has superhard and incompressibility properties, but only two publications have reported its chemical properties. In 2008, Levine et al.<sup>7</sup> reported a thermogravimetric analysis (TGA) of  $\text{ReB}_2$  in dry air showing an exothermic peak at 600 °C due to the volatilization of rhenium oxide ( $\text{ReO}_3$ ). While in 2011, Orlovskaya et al.<sup>13</sup> reported the formation of boric acid ( $\text{H}_3\text{BO}_3$ ) and perrhenic acid ( $\text{HReO}_4$ ) after  $\text{ReB}_2$  powder was exposed to oxygen and moisture ambient environmental conditions for one year. Therefore, a study about chemical properties of  $\text{ReB}_2$  should be a priority in order to verify if the  $\text{ReB}_2$  is a candidate material to be used for cutting, polishing and grinding tools at oxygen and moisture ambient environmental conditions. Here, we reported the mechanosynthesis of  $\text{ReB}_2$  and its chemical stability monitored for 26 months of storage at oxygen and moisture ambient environmental conditions. The stability study of the  $\text{ReB}_2$  sample indicates that it is decomposed at oxygen and moisture ambient environmental conditions and a schematic diagram of the degradation sequence is proposed and validated.

## 2. Experimental procedure

### 2.1. Synthesis and characterization of $ReB_2$

A 1:2 molar ratio mixture of rhenium (Sigma-Aldrich, 99.995%) and boron (Sigma-Aldrich, 99%) was placed in a mortar and mechanically treated with a pestle until a homogeneous powder was obtained. The mixture was transferred to a WC grinding jar (80 mL volume), using 15 balls of WC (10 mm in diameter). The grinding jar was placed in a planetary mill (Pulverisette 7, Fritsch, Germany). The ball milling was carried out at 600 rpm. Cycles of five min of milling and 12 min of pause were used to minimize the overheating. X-ray diffraction (XRD) patterns were immediately acquired at 640 and 800 min of milling time to monitor the reaction using a Bruker D8 Advance diffractometer. The morphology and microstructure were obtained using a scanning electron microscope (Quanta 200 ESEM, FEI) and a transmission electron microscope (HRTEM Tecnai F30, FEI).

### 2.2. Stability analysis of $ReB_2$

In order to carry out the stability study, the  $ReB_2$  powder that was obtained by mechano-synthesis was analyzed by XRD (SmartLab diffractometer, Rigaku) after two months that the powder was stored at oxygen and moisture ambient environmental conditions (average annual relative humidity: 59 %, average maximum temperature: 24.3 °C and average minimum temperature: 10.5 °C). From there, the powder was characterized by thermogravimetric analysis and differential scanning calorimetry (TGA-DSC) (SETARAM Evolution thermal analyzer, Setsys) from 50 to 1500 °C, using a heating rate of 10 °Cmin<sup>-1</sup> and an Ar flow of 20 mLmin<sup>-1</sup>. Infrared spectroscopy (Spectrum One model 59081, Perkin Elmer) and Raman spectroscopy (micro-Raman spectrometer, Renishaw) with 532 nm laser line. Finally, the powder was stored up to 26 months at oxygen and moisture ambient environmental conditions and it was analyzed by XRD and SEM using a scanning electron microscope (Quanta 250, FEI).

### 3. Results

#### 3.1. Characterization of $\text{ReB}_2$

The reaction was monitored by XRD during the milling process. The formation of  $\text{ReB}_2$  was observed after 640 min of milling. The XRD patterns of the samples at 640 and 800 min of milling are shown in Fig. 1. The diffraction patterns obtained after 640 min of milling are in good agreement with the diffraction pattern of hexagonal  $\text{ReB}_2$  (PDF4+ 00-011-0581). In both diffractograms (Fig. 1), no diffraction peaks from unreacted rhenium or boron were observed, and no signals from tungsten carbide from the milling media or another rhenium boride phase ( $\text{Re}_7\text{B}_3$ ,  $\text{Re}_3\text{B}$ ) were observed either. Therefore, the  $\text{ReB}_2$  mechanosynthesis methodology used in this study is faster and more efficient than the one reported by Orlovskaya et al.<sup>13</sup>

The morphology of the sample after 640 min of milling obtained by SEM is shown in Fig. 2. The micrographs show clusters of polyhedral particles as the characteristic morphology of  $\text{ReB}_2$  growth. A magnification from the white frame in Fig. 2a is shown in Fig. 2b where one octahedral-like micro-particle is observed. In order to establish the chemical nature of the polyhedral particles an EDS analysis was performed. The EDS spectrum, Fig. 2d, was collected from the white frame of Fig. 2c. The EDS spectrum indicates that the micro-particles are formed mainly by rhenium; the sensitivity of EDS is higher for heavy atoms than for light atoms such as boron whose concentration is generally underestimated or not estimated. Thus, considering the XRD results it can be concluded that the micro-particles are formed by  $\text{ReB}_2$ . The presence of oxygen (O) in the EDS spectrum could indicate oxidation on the  $\text{ReB}_2$  surface through the reaction with molecular oxygen and/or water. The gold (Au) peak is from the coating used to avoid accumulation charge on the sample.

Low magnification bright field images, obtained by transmission electron microscopy analysis are shown in Fig. 3. The average particle size of those nanoparticles is smaller than 50 nm, furthermore, those nanoparticles can be seen as the seeds for the formation of the polyhedral micro-particles of  $\text{ReB}_2$  shown in Fig. 2, and their nanometric size results from depletion of the reagents in the bowl of reaction. In order to evaluate the crystallinity of the  $\text{ReB}_2$  nanoparticles, HRTEM was used. HRTEM micrographs, Fig. 4, confirmed that the nanoparticles in Fig. 3 are  $\text{ReB}_2$ . The interplanar distances and angles are in good agreement with the  $\text{ReB}_2$  crystal structure (PDF4+ 00-011-0581); some Miller indices are also shown.

### *3.2. Stability of $\text{ReB}_2$ under oxygen and moisture ambient environmental conditions for 2 months*

As was mentioned previously, the EDS analysis of polyhedral particles of  $\text{ReB}_2$  in Fig. 2 shows the presence of oxygen as an indicative of possible  $\text{ReB}_2$  degradation at oxygen and moisture ambient environmental conditions. In order to verify this statement, an XRD analysis of the  $\text{ReB}_2$  sample after two months of storage at oxygen and moisture ambient environmental conditions was carried out. The obtained diffractogram is shown in Fig. 5 and the corresponding stick diagram for the following phases are shown:  $\text{H}_3\text{BO}_3$  (PDF4+ 00-009-0335),  $\text{ReO}_3$  (H, hexagonal phase; PDF4+ 00-040-1155) and  $\text{ReB}_2$  (PDF4+ 00-011-0581). From the XRD pattern it can be seen that the  $\text{ReB}_2$  obtained from mechanosynthesis is not a stable material at oxygen and moisture ambient environmental conditions. The formation of  $\text{ReO}_3$  is more evident than  $\text{H}_3\text{BO}_3$  after two months of storage at oxygen and moisture ambient environmental conditions. In order to obtain more information about the degradation sequence of  $\text{ReB}_2$  after two months of storage at oxygen and moisture ambient environmental conditions, TGA- DSC, FTIR and Raman analysis were performed on the sample. TGA-DSC results are shown in Fig. 6. The thermogram shows a first stage from 50 °C to 150 °C that is attributed to water evaporation and volatilization of  $\text{HReO}_4$

(liquid) from the surface of the sample, from 163 °C to 190 °C is attributed to dehydration of boric acid ( $\text{H}_3\text{BO}_3$ ) to form metaboric acid ( $\text{HBO}_2$ ) and from 190 °C to 350 °C is attributed to dehydration  $\text{HBO}_2$  to form  $\text{B}_2\text{O}_3$ .<sup>14-16</sup> From 420 °C to 1100 °C due to the decomposition of  $\text{ReO}_3$  into  $\text{ReO}_2$  and  $\text{O}_2$ .<sup>7,13,17,18</sup> The stage from 1130 °C to 1170 °C can be associated to vaporization of  $\text{HBO}_2$ .<sup>19</sup> The last stage of weight loss, from 1280 °C to 1500 °C, is due to the sublimation of  $\text{ReO}_2$  which has a boiling point of 1363 °C and vaporization of  $\text{B}_2\text{O}_3$ .<sup>17,19,20</sup> The total weight loss of the residue at 1500 °C was 76.6 % w/w, the major loss of weight is attributed to  $\text{ReO}_3$  material because the  $\text{ReB}_2$  is composed of 10.4 % w/w of B and 89.6 % w/w of Re. From the DSC curve (Fig. 6), three endothermic peaks at low temperature can be seen: water desorption at 110°C, the dehydration of boric acid to form metaboric acid ( $\text{HBO}_2$ ) at 163 °C and dehydration of  $\text{HBO}_2$  to form  $\text{B}_2\text{O}_3$  at 194 °C.<sup>14-16</sup> Subsequently, a broad exothermic peak was observed at 420 °C; this peak can be associated to the decomposition of  $\text{ReO}_3$  into  $\text{ReO}_2$  and  $\text{O}_2$ .<sup>17</sup> Finally, the last two endothermic peak can be assigned to vaporization of  $\text{HBO}_2$  and  $\text{B}_2\text{O}_3$  at 1150 °C and 1450 °C, respectively.<sup>19,20</sup>

The FTIR and Raman spectra of  $\text{ReB}_2$  stored two months under oxygen and moisture ambient environmental conditions are shown in Fig.7 and Fig. 8, respectively. The IR spectrum of the material shows several adsorptions peaks at 547  $\text{cm}^{-1}$  (B-O), 793  $\text{cm}^{-1}$  (B-O), 1193  $\text{cm}^{-1}$  (B-O), 1431  $\text{cm}^{-1}$  (B-OH), 3312  $\text{cm}^{-1}$  (B-OH) and 3406  $\text{cm}^{-1}$  (B-OH) which indicate the oxidation and the degradation of the surface of  $\text{ReB}_2$  particles due to the reaction with  $\text{O}_2$  and moisture.<sup>21-23</sup> Also, one absorption peak at 2260  $\text{cm}^{-1}$  (B-H) which indicates the reductive properties of  $\text{ReB}_2$  particles.<sup>22-24</sup> The absorption peak at 913  $\text{cm}^{-1}$  (Re-O) confirms the oxidative properties of this material.<sup>25,26</sup> A weak absorption peak at 642  $\text{cm}^{-1}$  (B-B) can be associated with the layered structure of  $\text{ReB}_2$ .<sup>4</sup> The Raman spectrum shows peaks at 208  $\text{cm}^{-1}$  (lattice oscillation), 500  $\text{cm}^{-1}$  (O-B-O)

and  $881\text{ cm}^{-1}$  (B-O), all attributed to vibration modes of  $\text{H}_3\text{BO}_3$ .<sup>27</sup> Peaks at  $338\text{ cm}^{-1}$ ,  $928\text{ cm}^{-1}$  and  $981\text{ cm}^{-1}$  correspond to symmetric and antisymmetric stretching modes of tetrahedral  $[\text{ReO}_4]^{-1}$  ion and other characteristic modes.<sup>28,29</sup>

### *3.3. Stability of $\text{ReB}_2$ under oxygen and moisture ambient environmental conditions for 26 months*

As shown in Fig. 5, XRD analysis indicates that  $\text{ReB}_2$  is unstable at oxygen and moisture ambient environmental conditions, which was corroborated by TGA-DSC, FTIR and Raman analysis. In order to evaluate further degradation the  $\text{ReB}_2$  sample was analyzed by XRD after 26 months of storage at oxygen and moisture ambient environmental conditions; the diffractogram is shown in Fig. 9. The diffractogram shows a mixture of different phases such as:  $\text{H}_3\text{BO}_3$ ,  $\text{ReO}_3$  (H, hexagonal),  $\text{ReO}_3$  (C, cubic phase; PDF4+ 04-004-8088) and  $\text{HBO}_2$  (PDF4+ 00-022-1109). No reflections from  $\text{ReB}_2$  are observed in the diffractogram. The SEM characterization of the same sample is shown in Fig. 10. Two different morphologies are observed by SEM analysis: plate-like micro-particles (Fig. 10a; white arrows) and irregular micro-particles (Fig. 10c). EDS spectrum from plate-like micro-particles (Fig. 10b) shows characteristic x-ray emission lines for B, O and Re that could indicate the presence of rhenium oxides, boric acid and metaboric acid. EDS spectrum from irregular micro-particles (Fig. 10c) shows characteristic x-ray emission lines for O and Re that could mainly indicate the presence of rhenium oxides. The final products of the  $\text{ReB}_2$  degradation are  $\text{H}_3\text{BO}_3$ ,  $\text{HBO}_2$  and  $\text{ReO}_3$ . The TGA analysis of the  $\text{ReB}_2$  sample after 26 months of storage at oxygen and moisture ambient environmental conditions is shown in Fig. 11. The thermogram is very similar to the thermogram showed in Fig. 6 can be seen several weight loss stages can be seen: from  $50\text{ }^\circ\text{C}$  to  $150\text{ }^\circ\text{C}$  which is attributed to water evaporation from the surface of the sample; from  $150\text{ }^\circ\text{C}$  to  $200\text{ }^\circ\text{C}$  which is attributed to dehydration of boric acid ( $\text{H}_3\text{BO}_3$ ) forming metaboric acid ( $\text{HBO}_2$ ); from  $200\text{ }^\circ\text{C}$  to  $300\text{ }^\circ\text{C}$  which is attributed to the dehydration of

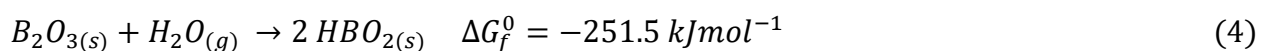
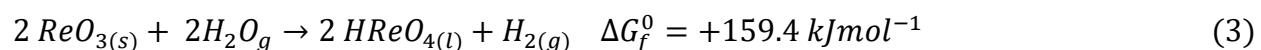
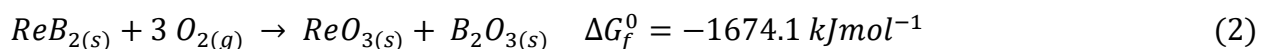
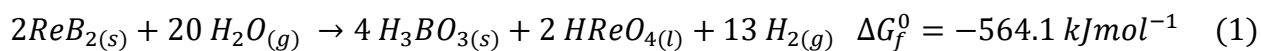


HBO<sub>2</sub> to form B<sub>2</sub>O<sub>3</sub> and from 400 °C to 1000 °C due to the decomposition of ReO<sub>3</sub> into ReO<sub>2</sub> and O<sub>2</sub>. The total weight loss of the residue at 1000 °C was 68 % w/w. XRD and SEM characterization of ReB<sub>2</sub> sample after 26 months of synthesis shows complete ReB<sub>2</sub> degradation at oxygen and moisture ambient environmental conditions.

#### 4. Discussion

Using the information obtained in sections 3.1-3.3, four equations were proposed to explain ReB<sub>2</sub> degradation at oxygen and moisture ambient environmental conditions. Thermodynamic values for each compound were obtained from the literature.<sup>30-34</sup> Thermodynamic analysis indicates that the equations (1, 2) and (4) are favored at environmental temperature, while the equation (3) is not favored at these conditions. These results are consistent with the stability analysis in sections 3.2 and 3.3 and revealed why the Re from ReB<sub>2</sub> is converted into ReO<sub>3</sub> and HReO<sub>4</sub> (liquid), while B is converted into H<sub>3</sub>BO<sub>3</sub> and HBO<sub>2</sub> at oxygen and moisture ambient environmental conditions. The formation of HBO<sub>2</sub> due to the hydration of B<sub>2</sub>O<sub>3</sub> (equation 2) in humid ambient air is a well-documented process.<sup>35-37</sup> Orlovskaya et al.<sup>13</sup> reported the degradation of ReB<sub>2</sub> into H<sub>3</sub>BO<sub>3</sub> and HReO<sub>4</sub>, through the formation of Re<sub>2</sub>O<sub>7</sub>; however our study shows that the degradation is through the formation of two ReO<sub>3</sub> polymorphs and liquid HReO<sub>4</sub>. Furthermore, the ReO<sub>3</sub> phases are very stable. Finally, using the information obtained in this section and the 3.1-3.3 sections, a diagram ReB<sub>2</sub> degradation under oxygen and moisture ambient environmental conditions is proposed, which is shown in Fig. 12. As we mentioned in the introduction of this paper, materials with high hardness, incompressibility and chemical inertness can be used in cutting and grinding tools. The ReB<sub>2</sub> has incompressibility behavior, but their superhard<sup>38</sup> and chemical inertness properties are under discussion in the scientific community. Conclusions of our paper indicates that ReB<sub>2</sub> is not a good material to make cutting tool because its degradation at oxygen and moisture ambient

environmental conditions compromises its superhard properties and limit its use in non-oxidative environment.



## 5. Conclusions

The mechanosynthesis of ReB<sub>2</sub> after 640 min of milling from rhenium and boron powders is reported. The stability study of ReB<sub>2</sub> after 26 months of storage at oxygen and moisture ambient environmental conditions indicates that the material is completely decomposed in the presence of O<sub>2</sub> and H<sub>2</sub>O; these results were supported by thermodynamic analysis of the ReB<sub>2</sub> degradation. A degradation diagram of ReB<sub>2</sub> at oxygen and moisture ambient environmental conditions is proposed. An inert protective atmosphere is recommended for safeguarding the integrity of ReB<sub>2</sub>.

## Acknowledgments

This work was supported by the Consejo Nacional de Ciencia y Tecnologia (CONACYT) under the grants LINAN-0271911 and FC-2015-2-947. The authors wish to acknowledge scholarship support from CONACYT for MGGF. The authors also acknowledge Hector Silva, Dulce Partida, Beatriz Rivera, Ana Peña, Ignacio Becerril, Matthew Tippett, the LINAN, the IPICYT, the UNPA and the UABC for providing laboratory support.

## References

- <sup>1</sup>Kanyanta V. Microstructure-Property Correlations for Hard, Superhard, and Ultrahard Materials. Switzerland: Springer;2016.
- <sup>2</sup> La Placa S, Post B. The crystal structure of rhenium diboride. *Acta Crystallogr.* 1962;15:97-99.
- <sup>3</sup> Zhou W, Wu H, Yildirim T. Electronic, dynamical, and thermal properties of ultra-incompressible superhard rhenium diboride: A combined first-principles and neutron scattering study. *Phys Rev B* 2007;76:184113.
- <sup>4</sup> Chung HY, Weinberger MB, Levine JB, et al. Synthesis of ultra-incompressible superhard rhenium diboride at ambient pressure. *Science.* 2007;316:436-439.
- <sup>5</sup> Chung HY, Weinberger MB, Yang JM, et al. Correlation between hardness and elastic moduli of the ultraincompressible transition metal diborides RuB<sub>2</sub>, OsB<sub>2</sub>, and ReB<sub>2</sub>. *Appl Phys Lett.* 2008;92:261904.
- <sup>6</sup> Qin J, He D, Wang J, et al. Is rhenium diboride a superhard material? *Adv Mater.* 2008;20:4780-4783.
- <sup>7</sup> Levine JB, Nguyen SL, Rasool HI, et al. Preparation and properties of metallic, superhard rhenium diboride crystals. *J Am Chem Soc.* 2008;130:16953-16958.
- <sup>8</sup> Latini A, Rau JV, Ferro D, et al. Superhard rhenium diboride films: preparation and characterization. *Chem Mater,* 2008;20:4507-4511.
- <sup>9</sup> Wang Y, Zhang J, Daemen LL, et al. Thermal equation of state of rhenium diboride by high pressure-temperature synchrotron x-ray studies. *Phy Rev B.* 2008, 78, 224106
- <sup>10</sup> Koehler MR, Keppens V, Sales BC, et al. Elastic moduli of superhard rhenium diboride. *J Phys D Appl Phys.* 2009;42:095414.

- <sup>11</sup> Arellano EAJ, Winkler B, Friedrich A, et al. In situ study of the formation of rhenium boride from the elements at high-(p,T) conditions: extreme incompressibility of  $\text{Re}_7\text{B}_3$  and formation of new phases. *Solid State Sci.* 2013;25:85-92.
- <sup>12</sup> Chrzanowska J, Hoffman J, Denis P, Gizynski M, Moscicki T. The effect of process parameters on rhenium diboride films deposited by PLD. *Surf Coat Technol.* 2015;277:15-22.
- <sup>13</sup> Orlovskaya N, Xie Z, Klimov M, et al. Mechanochemical synthesis of  $\text{ReB}_2$  powder. *J Mater Res.* 2011;26:2772-2779.
- <sup>14</sup> Kocakuşak S, Köroğlu HJ, Tolun R. Drying of wet boric acid by microwave heating. *Chem Eng Process.* 1998;37:197-201.
- <sup>15</sup> Sevim F, Demir F, Bilen M, et al. Kinetic analysis of thermal decomposition of boric acid from thermogravimetric data. *Korean J Chem Eng.* 2006;23:734-738.
- <sup>16</sup> Balci S, Sezgi NA, Eren E. Boron oxide production kinetics using boric acid as raw material. *Ind Eng Chem Res.* 2012;51:11091-11096.
- <sup>17</sup> Bai M, Liu Z, Zhou L, et al. Preparation of ultrafine rhenium powders by CVD hydrogen reduction of volatile rhenium oxides. *Trans Nonferrous Met Soc China.* 2013;23:538-542.
- <sup>18</sup> Wei J, Bai D, Yang L. Polymer photovoltaic cells with rhenium oxide as anode interlayer. *Plos ONE.* 2015;10:1-8.
- <sup>19</sup> Steinbrück M. Oxidation of boron carbide at high temperature. *J Nucl Mat.* 2005;336:185-193.
- <sup>20</sup> Zhang XH, Hu P, Han JC. Structure evolution of  $\text{ZrB}_2\text{-SiC}$  during the oxidation in air. *J Mater Res.* 2008;23:1962-1972.
- <sup>21</sup> Wang Y, Xue X, Yang H. Preparation and characterization of carbon or/and boron-doped titania nano-materials with antibacterial activity. *Ceram Int.* 2014;40:12533-12537.

- <sup>22</sup>Tsou HT, Kowbel W. Design of multilayer plasma-assisted CVD coatings for the oxidation protection of composite materials. *Surf Coat Tech.* 1996;79:139-150.
- <sup>23</sup>Shin WG, Calder S, Ugurlu O, et al. Production and characterization of boron nanoparticles synthesized with a thermal plasma system. *J Nanopart Res.* 2011;13:7187-7191.
- <sup>24</sup>Deshpande SV, Gulari E, Harris SJ, et al. Filament activated chemical vapor deposition of boron carbide coatings. *Appl Phys Lett.* 1994;65:1757-1759.
- <sup>25</sup>Uscategui AV, Mosquera E, Encarnacion JML, et al. Characterization of rhenium compounds obtained by electrochemical synthesis after aging process. *J Solid State Chem.* 2014;220:17-21.
- <sup>26</sup>Ayvali T, Lecante P, Fazzini PF, et al. Facile synthesis of ultra-small rhenium nanoparticles. *Chem Commun.* 2014;50:10809-10811.
- <sup>27</sup>Krishnan K. The Raman spectrum of boric acid. *Proc Indian Acad Sci.* 1963;57:103-108.
- <sup>28</sup>Cazzanelli E, Castriota M, Marino S, et al. Characterization of rhenium oxide films and their application to liquid crystal cells. *J Appl Phys.* 2009;105:114904.
- <sup>29</sup>Purans J, Kuzmin A, Cazzanelli E, et al. Disorder-induced Raman scattering in rhenium trioxide (ReO<sub>3</sub>). *J Phys Condens Matter.* 2007;19:226206.
- <sup>30</sup>Colinet C, Tedenac JC. Enthalpies of formation of transition metal diborides: a first principles study. *Crystals.* 2015;5:562-582.
- <sup>31</sup>Guillermet AF, Grimvall G. Bonding properties and vibrational entropy of transition metal MeB<sub>2</sub> (AlB<sub>2</sub>) diborides. *J Less Common Met.* 1991;169:257-281.
- <sup>32</sup>Dean JA, Lange NA. Lange's handbook of chemistry. 15th ed. USA: McGraw-Hill; 1999.
- <sup>33</sup>Stuve JM, Ferrante MJ. "Thermodynamics properties of rhenium oxides, 8 to 1400 K". USA: Albany Metallurgy Research Center, Department of the interior, Bureau of Mines; 1976.

<sup>34</sup> Wang P, Kosinski JJ, Lencka MM, et al. Thermodynamic modeling of boric acid and selected metal borate systems, *Pure Appl Chem*. 2013;85:2117-2144.

<sup>35</sup> Kracek FC, Morey GW, Merwin HE. The system water-boron oxide. *Am J Sci*. 1938;235A:143-171.

<sup>36</sup> Berger SV. The crystal structure of B<sub>2</sub>O<sub>3</sub>. *Acta Crystallogr*. 1952;5:389.

<sup>37</sup> Gogotsi YG, Lavrenko VA. Corrosion of High-Performance Ceramics. Germany; Springer Science and Business Media: 2012.

<sup>38</sup> Dubrovinskaia N, Dubrovinsky L, Solozhenko VL. Comment on “Synthesis of Ultra-Incompressible Superhard Rhenium Diboride an Ambient Pressure”. *Science*. 2007;318:1550.

**Figure 1. XRD patterns of ReB<sub>2</sub> obtained at 640 and 800 min of milling. The diffraction patterns were collected immediately after the milling process. The sticks plot corresponds to hexagonal ReB<sub>2</sub> (PDF4+ No. 00-011-0581).**

**Figure 2. SEM micrographs of the sample obtained at 640 min of milling. (a) Cluster of micro-particles, (b) a magnification showing a polyhedral particle, (c) cluster of micro-particles and (d) EDS spectra from the white frame in (c).**

**Figure 3. Low magnification TEM micrographs of particles from the sample obtained at 640 min of milling.**

**Figure 4. HRTEM micrographs of the sample obtained at 640 min of milling. Crystalline ReB<sub>2</sub> nanoparticles are observed.**

**Figure 5. XRD pattern of ReB<sub>2</sub> after two months of its synthesis. The bars correspond to each phase observed in the sample.**

**Figure 6. TGA-DSC analysis of ReB<sub>2</sub> after two months of storage at oxygen and moisture ambient environmental conditions.**

**Figure 7. FTIR spectra of the ReB<sub>2</sub> sample after two months of storage at oxygen and moisture ambient environmental conditions.**

**Figure 8. Raman Spectrum from the sample of ReB<sub>2</sub> after two months of storage at oxygen and moisture ambient environmental conditions.**

**Figure 9. XRD pattern of ReB<sub>2</sub> after 26 months of storage at oxygen and moisture ambient environmental conditions. Several phases in the diffractogram are observed. No reflections from the starting phase of ReB<sub>2</sub> is observed.**

**Figure 10. SEM characterization of ReB<sub>2</sub> sample after 26 months storage at oxygen and moisture ambient environmental conditions. (a) and (c) Cluster of micro-particles, (b) and (d) EDS spectra from white frames in (a) and (c), respectively.**

**Figure 11. TGA analysis of ReB<sub>2</sub> after 26 months of storage under oxygen and moisture ambient environmental conditions.**

**Figure 12. Schematic diagram of the proposed degradation sequence of ReB<sub>2</sub> at oxygen and moisture ambient environmental conditions.**